

On stress drops in the sources of moderate and weak earthquakes: features of distribution in time

Leonid M. Bogomolov¹, Vladimir N. Sychev*¹, Naylya A. Sycheva²

*E-mail: koitash@mail.ru

¹Institute of Marine Geology and Geophysics, FEB RAS, Yuzhno-Sakhalinsk, Russia

²Schmidt Institute of Physics of the Earth of RAS, Moscow, Russia

Abstract. An analysis has been performed of the change in stress drops over time during the period of foreshock activity of strong earthquakes for two seismically active regions with different geodynamic settings: the Northern Tien Shan and the Southern Kuril Islands. The catalogs of earthquake dynamic parameters, DP (source ones in English publications), in these regions, with a number of events, were used as initial data. The DP catalog for the Northern Tien Shan includes 183 records of source parameters of earthquakes with magnitudes of 2.6–6.0, and the catalog for the Southern Kurils – 264 records. The stress drop values throughout a general sampling were analyzed as well as that in foreshock periods of 500 days length before the strongest earthquakes. For each region 12 such meaningful events have been specified, the magnitudes were $M > 5$ for the Northern Tien Shan, and $M \geq 6.5$ for the Southern Kurils. The median average values of stress drops during 500-day period have been determined. The temporal variations of stress drops have been compared with changes in the b -value parameter (angular coefficient of earthquake recurrence plot) in the same observation periods. The computation of b -value for the case of the Northern Tien Shan involved the catalog data of KNET seismological network (1994–2021, more than 10 000 events), and the catalog of International Seismological Center (ISC, 1964–2000) for the Southern Kurils. In both cases, b -values were determined in 500-day moving interval with one day step. The computation gave the result that the well-known effect of b -value growth before strong earthquakes manifested itself explicitly in the considered regions. It has been established that such increase in b -value is accompanied by a decrease in the averaged stress drop values. The obtained results showed that the monitoring of the stress drop values can be used to identify the non stationary stage of the seismic regime.

Keywords: earthquake, seismicity, foreshocks period, stress drops, b -value, Northern Tien Shan, Southern Kuril Islands

For citation: Bogomolov L.M., Sychev V.N., Sycheva N.A. On stress drops in the sources of moderate and weak earthquakes: features of distribution in time. *Geosistemy perhodnykh zon = Geosystems of Transition Zones*, 2023, vol. 7, no. 1, pp. 25–53. (In Russ. & Engl.). <https://doi.org/10.30730/gtrz.2023.7.1.025-036.037-053>; <https://www.elibrary.ru/xdworg>

Acknowledgements and funding

The work was carried out within the framework of the state task of the Institute of Marine Geology and Geophysics FEB RAS (no. 121022000085-9) and the state task of the Schmidt Institute of Physics of the Earth of RAS (no. 122040600089-4).

Introduction

Recent works [1] have demonstrated the possibility and feasibility of mass determination of dynamic parameters (DP) of earthquake sources in the case of seismically active regions where modern seismological networks are deployed.

For such regions, the computation of DP values allows creating the DP data banks with a sufficiently large number of records comparable to the number of accumulated seismic events during the same observation period. This, in turn, enhances the ability to describe regional features of the geodeformation process. DP includes the scalar seismic moment M_0 , the source radius r (defined, in particular, according to the Brune's model [2–6] or alternative models [7]), as well as the tangent

stress drop $\Delta\sigma$ and the specific seismic energy, representing the ratio of the radiated seismic energy E_s to the seismic moment M_0 : $e_{PR} = E_s/M_0$.

It is worth noting that the traditional point of view is still popular, according to which it makes sense to define and consider dynamic parameters only for strong earthquakes [2–4, 8]. However, the importance of a statistically relevant DP dataset has been clearly highlighted in the fundamental question of the existence of the earthquake source self-similarity. As argued in [9–12], the sign of self-similarity is the absence of regression between the values of the specific seismic energy (or proportional e_{PR} values of stress drops). In our previous works [7, 13], approximate dependencies (regressions) were identified between stress

drops $\Delta\sigma$ and the scalar seismic moment M_0 for two seismic regions of Northern Eurasia with different geodynamic settings – the Northern Tien Shan and the Northwest Pacific. In this case, the values $\Delta\sigma$ and M_0 from the earthquake dynamic catalogs for the Northern Tien Shan [1, 7, 14] and the Northwest Pacific [3] were considered for the respective observation periods.

A natural continuation of the statistical analysis of $\Delta\sigma$ values from [1, 7] is the search of time features of stress drop distributions. Are there the periods when the relationships between $\Delta\sigma$ and M_0 are different from those identified over the entire catalog? This paper attempts to answer this question. Presumably, the features of stress drop distribution appear primarily during the periods of foreshock and aftershock activation. Therefore, our work pays attention to the values of stress drops during the preparation of significant earthquakes, when the features of $\Delta\sigma$ distribution can manifest themselves more contrastively.

Seismically active regions with different geodynamic settings have been selected for analysis: the Tien Shan, that is an intracontinental orogenesis region, the Northwest Pacific (the Southern Kuril Islands region), that is a subduction zone. A regular earthquake catalog and mass determination of earthquake dynamic parameters are important condition for research purposes. Such datasets are available for both regions. This will allow testing the hypothesis of reduction of the stress drop value during the preparation of earthquakes and also to determine its dependence on the type of geodynamic setting.

Study object and data used

The Northern Tien Shan

The Northern Tien Shan is a region of modern intensive deformations. The main tectonic forces in the region are due to the collision between the Indian and Eurasian plates, which determine the seismic activity in the region [15].

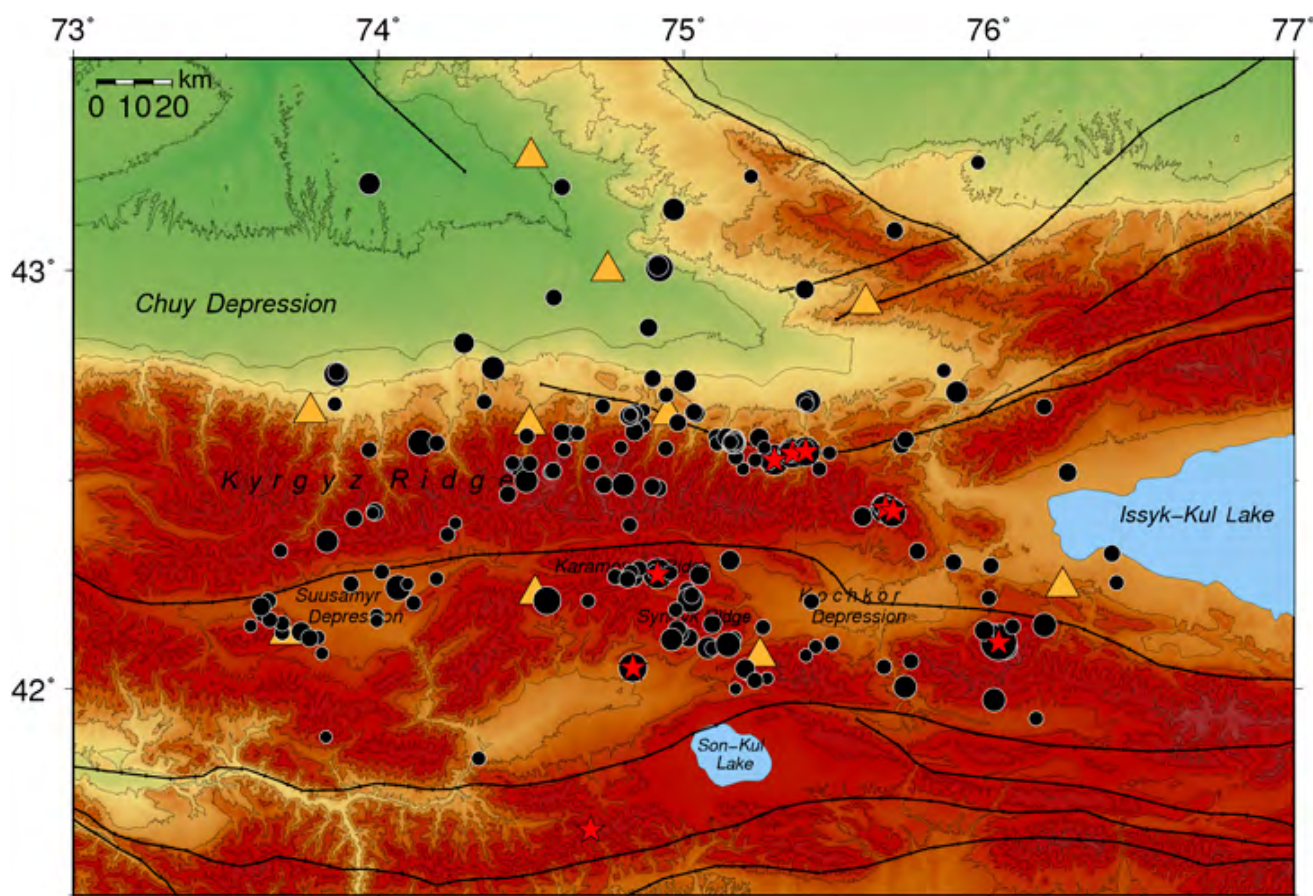


Fig. 1. Epicentral location of earthquakes (183 events), for which DP were computed. Triangles are the position of the stations of the KNET network. Black lines are regional faults. The minimum circle corresponds to an event with $M = 2.7$, the maximum – with $M = 6.0$. Red stars are events with $M > 5$, information about which is given in Table 1.

Table 1. Parameters of earthquakes with $M > 5$ in the Northern Tien Shan according to the data of the KNET network for the period of 1998–2017

No.	Date	Time	φ° , N	λ° , E	h , km	K	M	$\Delta\sigma$, MPa	$Me(\Delta\sigma_i)$, MPa	N
1	22.05.2003	18:11:55.01	42.989	72.814	7.0	14.26	5.7	N/D	4.71	9
2	16.01.2004	09:06:17.90	42.549	75.297	14.0	13.68	5.4	54.82	3.42	15
3	02.06.2004	17:15:10.82	42.276	74.914	17.9	13.25	5.1	N/D	3.42	19
4	08.11.2006	02:21:26.94	42.565	75.356	18.6	13.37	5.2	44.61	4.01	21
5	25.12.2006	20:00:58.32	42.112	76.032	0.1	14.83	6.0	631.66	3.48	22
6	06.06.2007	11:09:25.58	42.569	75.400	13.0	13.25	5.1	33.06	3.17	16
7	02.03.2010	01:55:36.02	42.433	75.661	19.3	13.34	5.2	109.21	3.42	18
8	09.04.2011	12:30:25.45	42.051	74.834	6.3	13.20	5.1	5.28	6.21	8
9	05.02.2012	07:10:15.20	41.396	74.761	13.4	13.21	5.1	N/D	8.50	8
10	23.11.2013	09:42:6.75	42.427	75.687	9.9	13.46	5.3	88.79	7.84	11
11	17.11.2015	17:29:36.61	40.426	73.187	3.1	13.53	5.3	N/D	6.58	12
12	07.12.2015	08:30:53.22	41.660	74.695	15.9	13.60	5.3	N/D	7.80	13

The KNET (Kyrgyz Network) seismic network, that consists of ten digital broadband stations (Fig. 1) and allows recording local and regional seismicity [1], is located on the territory of the Northern Tien Shan. To date, the earthquake catalog obtained from the data of the KNET network (KNET catalog) includes more than 10 thousand seismic events, that have occurred in 1994–2021. Some characteristics of the earthquake catalog and seismic process are given in the work [16].

The values of dynamic parameters of the sources for 183 earthquakes of different energy classes ($K = 8.7$ – 14.8 , $M = 2.6$ – 6.0), which had occurred during the period of 1998–2017 (Fig. 1), were obtained in the work [7]. Most of the earthquake epicenters are located on the northern slopes of the Kyrgyz Ridge, the Karamoynok Ridge, Sandyk Mountain and in the area of Suusamy and Kochkor depressions.

A sample of events with $M > 5$ occurred in the study area in 1998–2017 was formed from the KNET catalog. The choice of this magnitude threshold is due to the fact that no events occurred with $M \geq 6$ during the network operation, except for the 25 December, 2006 $M = 6.0$ Kochkor earthquake. Thus, a working catalog of 12 «test» events (Table 1) was compiled. In addition to the parameters of the 12 most powerful earthquakes, the table shows the number of events, N_i , falling into the 500-day period before the main event i , and the median value of stress drops $Me(\Delta\sigma_i)$, determined

by N_i events. These medians are used further to detect regular $\Delta\sigma$ changes prior to strong earthquakes.

The events that had been occurred in the territory, bounded by the coordinates of edge stations of the KNET network, and its immediate surroundings were considered when computing the earthquake dynamic parameters for the Northern Tien Shan. This is due to the aim to minimize the influence of the direction of the earthquake source when constructing the source spectrum by several stations of the KNET network [7].

The earthquakes of significant magnitude that were not included in the table also occurred in the study region: the 22 May, 2003 $M = 6.3$ Lugovskoye [17]; the 14 November, 2014 $M = 5.5$ Kajy-Say [18]; the 28 January, 2013 $M = 6.1$ Karkyra-Saraja; the 23 November, 2013 $M = 5.2$ Ulaholskoye [19]. These events had occurred at a distance from the area for which dynamic parameters of earthquakes are defined, so their foreshock activity was not analyzed in this study.

The Southern Kuril Islands

The Kuril-Kamchatka subduction zone is one of the most seismically active regions of Northeastern Eurasia, where the rate of subduction of the Pacific lithospheric plate under the North American and Okhotsk ones reaches 8 cm/year [20]. Interaction of lithospheric plates is accompanied by tectonic deformations, which appear both at the plate boundary and in its vicinity [21]. Earthquakes are most active along the Kuril island arc, with the vast majority occurring at depths of up to 100–150 km

with maximum seismic activity at depths of about 30–40 km. The high level of seismic activity in the area of the Kuril Islands is confirmed by the long-term statistics of recorded seismic events. On average, an earthquake with a magnitude of $M = 4.0$ occurs here every three days, with $M = 5.0$ – approximately once a month, with $M = 6.0$ – every six months, and with $M = 7.0$ – every two years. Catastrophic earthquakes with $M = 8.0$ or more occur every 10 years, on average [22].

The present work focuses on the area around the Southern Kuril Islands, bounded by coordinates 42° – 46° N, 144° – 151° E. Dynamic parameters of the sources in the northwestern part of the Pacific Ocean for the period of 1969–1996 for an area within 42 – 51° N, 140 – 159° E [3] were used to analyze the dependence of stress drop in the sources on time. This catalog was compiled by R.N. Burymskaya according to the data of analog (frequency-selective) seismic stations. It remains unique today as it includes dynamic parameters (including stress drop values) for 431 earthquakes, which is significantly greater compared to other regional DP catalogs. 264 events (Fig. 2) from the catalog [3] fall into the area of our interest around the Southern Kuril Islands. The information

about the hypocenters and dynamic parameters of these events is given in Table in the Appendix. The stress drop values given in [3] for the Brune's model are recalculated to the Madariaga model.

Interest to this area is also due to the 4 October, 1994 $M_w = 8.3$ Shikotan earthquake, which is one of the strongest seismic events in the world at the end of the 20th century. It is worth noting that in recent works dedicated to the earthquakes in Sakhalin-Kuril region, attention is generally focused on the seismic moment tensor computations [23], and there are no assessments of stress drops.

A catalog of earthquakes (12 320 events) that occurred in the territory of Sakhalin and the Kuril Islands (25° – 60° N, 130° – 170° E) from 01.01.1964 to 31.12.2000 was received from the ISC seismological center to analyze the foreshock activity of strong earthquakes in the Southern Kurils (42° – 46° N, 144° – 151° E).

Since the regions of the Northern Tien Shan and the Northwest Pacific differ in seismic settings, the thresholds for selecting the «test» earthquakes for them are different: it is defined at $M \geq 6.5$ level for the Southern Kuril Islands. If we take the threshold value $M > 5.0$ as for the Northern Tien Shan, then the catalog will consist of more than

1 000 events, with a large number of overlapping time intervals, that complicates the analysis. Thus, a sample of 12 earthquakes with $M \geq 6.5$ was formed from the ISC catalog. The epicenters of these earthquakes are marked by red stars in Fig. 2, and some of their parameters are given in Table 2. The Moneron and Shikotan earthquakes, which will be discussed in more detail below, are highlighted in color.

Methodology

The earthquake dynamic parameters can characterize not only the source area, but also the change (shear stress drop, $\Delta\sigma$) in the geodynamic regime of the seismically active region. In this regard, the variations of $\Delta\sigma$ during the period of foreshock activity are interesting.

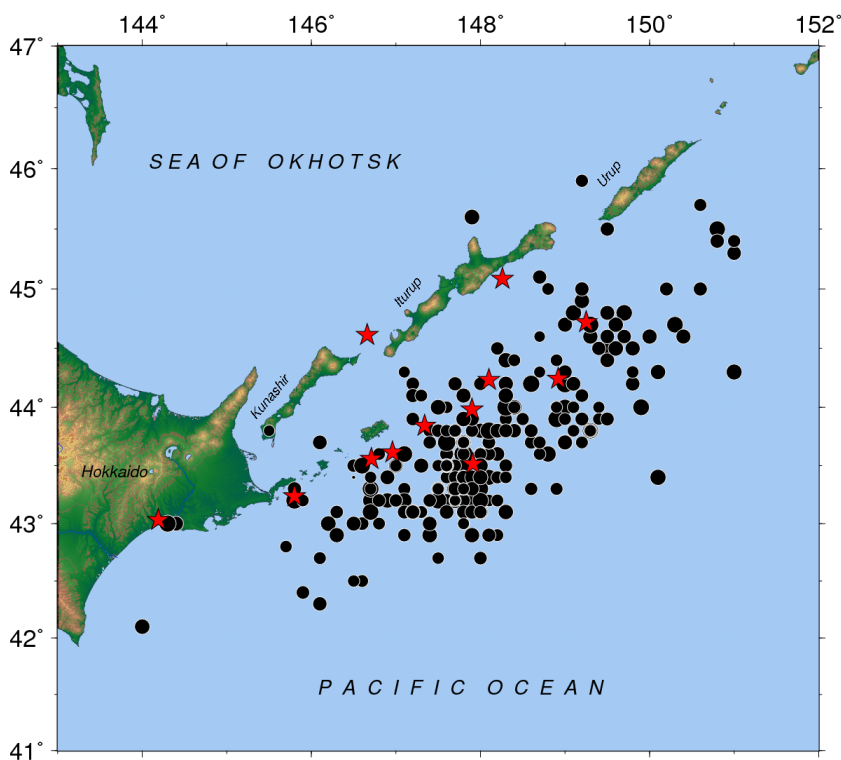


Fig. 2. Epicentral location of earthquakes in the Southern Kuril Islands with computed dynamic parameters (264 events) from the catalog [3]. Red stars are the events with $M \geq 6.5$ from the ISC catalog [24] (Table 2).

Table 2. Parameters of earthquakes with $M \geq 6.5$ in the region of the Southern Kuril Islands according to the ISC data for the period of 1969–1996

No.	Date	Time	φ° , N	λ° , E	h , km	M	$\Delta\sigma$, MPa	$Me(\Delta\sigma)$, MPa	N
1	11.08.1969	21:27:36.11	43.514	147.915	28.6	8.2	4.97	10.39	3
2	05.09.1971	18:35:28.52	46.559	141.174	18.1	7.5	N/D	14.67	11
3	17.06.1973	03:55:3.01	43.236	145.796	35.0	7.8	197.92	18.70	8
4	23.03.1978	03:15:21.65	45.085	148.257	25.0	7.7	62.59	19.81	10
5	24.03.1978	19:47:49.27	44.243	148.916	12.3	7.8	73.54	21.47	18
6	06.12.1978	14:02:5.85	44.613	146.656	120.5	7.8	N/D	5.98	34
7	03.09.1981	05:35:46.49	43.614	146.961	47.3	6.8	140.12	32.85	2
8	03.12.1984	04:08:35.88	44.233	148.102	59.4	6.5	41.35	15.72	1
9	15.01.1993	11:06:7.48	43.031	144.186	98.8	6.8	N/D	16.85	7
10	04.10.1994	13:23:0.44	43.842	147.340	35.0	7.9	N/D	7.35	29
11	09.10.1994	07:55:41.18	43.981	147.900	33.1	7.0	N/D	7.35	29
12	03.12.1995	18:01:10.18	44.721	149.247	30.0	7.6	279.58	5.64	6

The method of dynamic parameters computation is given in classical works [25, 26]. The computation results of dynamic parameters of the earthquakes in the Northwest Pacific are presented in [3]. The adaptation and application of this methodology for the Northern Tien Shan are covered in detail in [1, 7].

Two models are most often used to determine dynamic parameters of the source on the base of spectrum parameters: Brune's model [5, 6] and Madariaga one [27, 28]. The work [4] also provides a well-reasoned comparison of the models. We will briefly review the main features of using one or the other model.

In both models, a k coefficient is used to compute the source radius. It is a numerical coefficient that depends on the rupture model in a source. The choice of the k coefficient can significantly affect the error of the computation of the source radius value and, as a consequence, the stress drops.

In the work [5] the value of the k coefficient is determined on the basis of the simplest model of the source movement (the source zone is considered to be a ball with the radius r), and the shift of «hemispheres», b , along the rupture plane occurs immediately over the entire surface, bounded by the radius r , and $b \ll r$. The [5] computation gave $k = 0.37$ for this model, which is called the Brune's model and commonly used in the 20th century and in the zero years of 21st century.

However, the subsequent studies [29–33] have paid attention to the fact, that the values of

the source radius, based on the simplest model, turn out to be overestimated, in particular, when compared to the observations of a rupture breaking the ground surface. As a result, the estimates of stress drop may be several times lower than the actual values [30]. Models describing a coseismic displacement, i.e. the source mechanism, have been developed more adequately in [27, 28, 32, 34–36]. But the Brune's model, as noted in [1], can still be used, for example, when comparing the computations of dynamic parameters with the previously obtained results for a given region.

In the Madariaga model [27, 28], a disk rupture is considered as a source of seismic waves, the radius of which increases at a constant rate of V_R until it reaches a maximum value, r_M , identified with the source radius (radius of destruction, in the terms of [27]). No further growth of the crack occurs. In this model, the angular frequency depends on both the source radius and the V_R rupture rate, for which, according to [30, 32, etc.] the approximate value of $V_R \approx 0.9 \cdot V_S$ is generally accepted, where V_S is the rate of the S -wave. At this fracture rate, the coefficient k for the Madariaga model turns out to be $k = 0.21$. Due to the difference in k values, the source radius in the Brune's and Madariaga models differs by 1.76 times ($r = 1.76 r_M$). But the stress drop values for these models differ by about 5 times, since $\Delta\sigma \sim 1/r^3$. In other studies [32, 34–37], where the refinements of the Madariaga model or alternative models were analyzed, the computed values of the

source radius and stress drops are approximately in between their values in the Brune's and Madariaga models. In this case, the result obtained by Kaneko and Shearer [32], who were able to significantly improve the Madariaga model, can be considered to be important. According to [32], the k coefficient is 0.26 at the same rupture rate of $0.9 \cdot V_s$. In the case of this model, the source radius is 24 % larger than for the Madariaga model [27, 28], and stress drop is 1.9 times less than for the Madariaga model, but 2.9 times more than for the Brune's model. Our work uses an improved Madariaga–Kaneko–Shearer model [32].

The Gutenberg–Richter law [38] expresses the relationship between the magnitude and total number of earthquakes in any given region and time period. This law is described by a linear function of the form: $\lg N(M) = a - b \cdot M$, where $N(M)$ is the number of earthquakes with magnitudes (or classes) of at least that M , and a and b are equation constants. The parameter a (a -value) formally describes seismic activity when $M = 0$, and the b (b -value) is a slope of the linear part of the earthquake frequency distribution plot, which determines the rate of decrease in the relative number of events as their magnitude increases. The function $N(M)$ is computed to construct the Gutenberg–Richter distribution. This function graph is plotted on a logarithmic scale: the number of earthquakes $\lg N$ on magnitude M . Then we determine M_c – the minimum magnitude above which all earthquakes within a certain region are reliably recorded, M_{\max} – the maximum magnitude, for which enough events for statistics have occurred during the study time period. Further the plot interval ($M_c < x < M_{\max}$) of $y = \lg N(x)$ is approximated by a function of the form $y = a - b \cdot x$; b -value is used as an assessment of the statistical parameters of the seismic regime [39, 40]. The parameters of the linear part of the Gutenberg–Richter distribution – a -value and b -value – refer to the most important quantitative characteristics of the seismic regime. The slope of the graph expresses the ratio between the number of strong and weak seismic events, or (already in physical interpretation) the ratio between the number of large and small ruptures in the geological medium. The level of the graph characterizes seismic activity – the total intensity of seismic manifestations on the study seismic active area.

The work considers the behavior of the b -value parameter in the dynamics. Since the seismic event flow is a non-stationary process with significant fluctuations, a sufficient number of events are required to reliably determine the slope of the recurrence plot. Therefore, the b -value parameter was determined for a time interval of 500 days, or ~ 1.5 years. The b -value found was associated with the middle of the interval. Then the window was moved by one day, and the computation procedure was repeated. The beginning and end of the considered time intervals were determined according to the available catalogs of dynamic parameters: for the Northern Tien Shan from 26.08.1998 to 29.07.2017, for the zone of the Southern Kuril Islands from 18.03.1969 to 17.08.1996.

Taking into account the fact, that the stage of earthquake preparation is slow, as it reflects the process of geological transformation of the planet, a time window of 500 days before the event and 50 days after it was formed to detail the obtained time history of b -value close to large events. In the same window, the change in stress drops $\Delta\sigma$ was estimated: the median average value $Me(\Delta\sigma_{\text{all}})$ over the entire sample was determined and compared to the computed value $Me(\Delta\sigma_i)$ in the period preceding the earthquake (500 days).

Results

The histograms of stress drops $\Delta\sigma$ and change in the b -value in time were constructed for the study regions both for the entire interval under review, and for the time intervals close to the separate large events. Let us review the results obtained for each region.

The Northern Tien Shan

Result obtained for the Northern Tien Shan is presented in Fig. 3. The median average of stress drops over all events is marked ($Me(\Delta\sigma_{\text{all}}) = 5.0$ MPa).

The $\Delta\sigma$ value over the entire sample varies between 0.65 and 631.66 MPa. For better visualization of the graph in the area of small stress drop values, the upper limit on the $\Delta\sigma$ axis is constrained by 15.0 MPa.

Most of the events with $M > 5$ shown in the diagram occur during the periods of the b -value increasing, which may indicate a redistribution of events in favor of low-energy earthquakes. The obtained result fully corresponds to the pub-

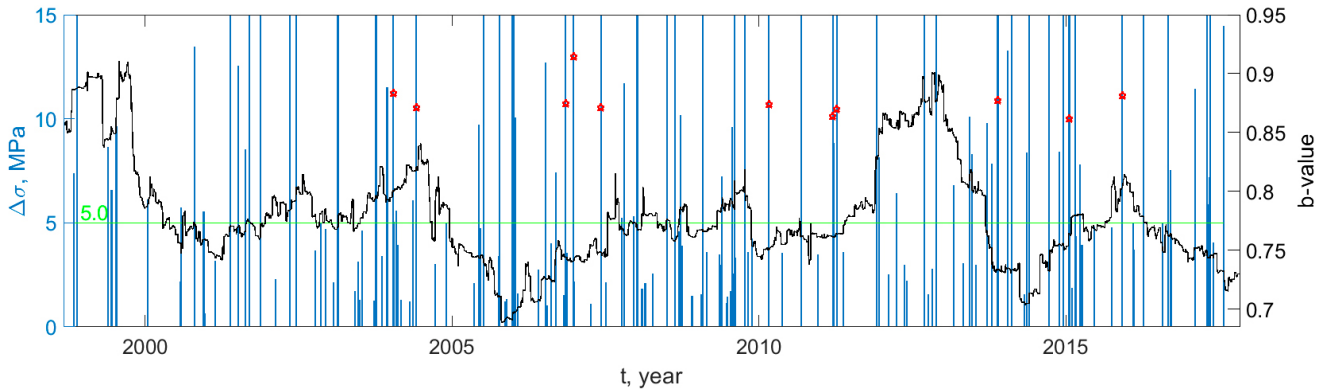


Fig. 3. The Northern Tien Shan. Histogram of stress drops in earthquake sources over time for the period of 1998–2017 (183 events) and the change in the b -value parameter for the considered time interval. Red stars are events with $M > 5$ from Table 1. Green line is the median average stress drops over all events.

lished one in [41] on the base of seismic observations at the Garm site in Republic of Tadjikistan, where studies of the b -value time variations revealed the phenomena, when large events preceded by anomalies associated with increasing in the slope of the recurrence graph.

Let us present the results for some separate earthquakes. For this purpose, we take the event of 02.06.2004 with $M = 5.1$ (no. 3 in Table 1) from the sample, which magnitude is close to the threshold $M > 5$, and the strongest one, the earthquake of 25.12.2006 with $M = 6.0$ (Kochkor earthquake, no. 5 in Table 1). Fig. 4 shows the distribution of $\Delta\sigma$ and the b -value for a time period of 500 days before and 50 days after the earthquakes. Note some features that are characteristic of both events.

First, in the foreshock period, the b -value gradually increases, which means an increase in the percent of the earthquakes of small energy classes. The second, the median average value

of stress drops computed in the interval average of 500 days till the selected event, $Me(\Delta\sigma_i)$, is less than the median average value of $\Delta\sigma$ over all 183 events throughout the entire time period.

The use of the median average value of some parameter, including $\Delta\sigma$, rather than the arithmetic mean or weighted mean, is standard when the values of this parameter differ radically in a statistical ensemble by several orders of magnitude [42]. The median describes the typical value of a parameter, around which most of the values in the sample are grouped.

The median average value of stress drops ($Me(\Delta\sigma_i) = 3.42$ MPa for the event no. 3 turned out to be 30 % less, then the median average value of $\Delta\sigma$ throughout all 183 events over the entire period ($Me(\Delta\sigma_{all}) = 5.0$ MPa. Despite the fact, that a large earthquake occurred on 08.11.2006 with $M = 5.2$ (no. 4 in Table 1) just before the Kochkor one and the values of stress drops for this

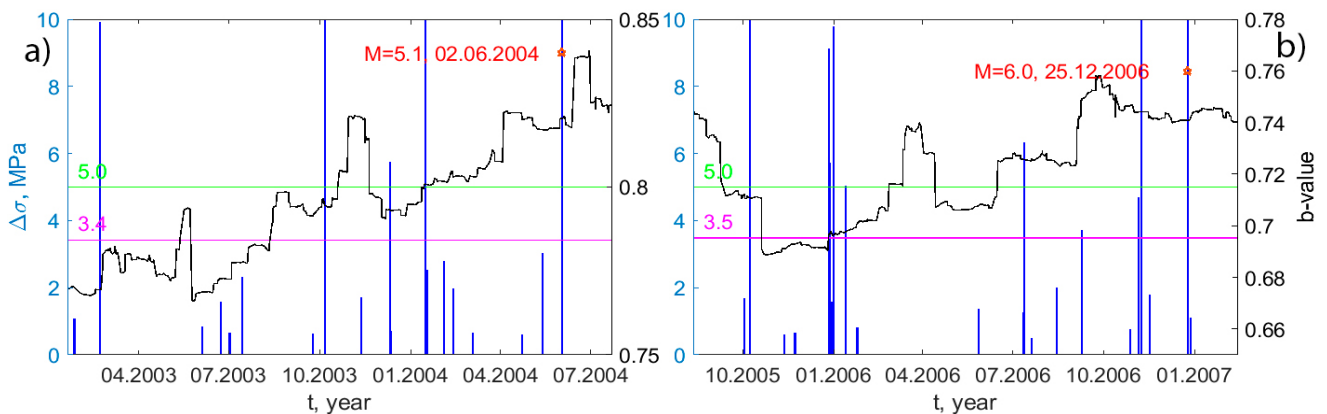


Fig. 4. Stress drop histogram before the event of 02.06.2004 with $M = 5.1$ (no. 3 in Table 1) (a) and the event of 25.12.2006 with $M = 6.0$ (no. 5 in Table 1) (b); the change in the b -value parameter. Green line is the median average value of stress drops for all events, the crimson line is the median value of stress drops for the events before the earthquake. Selected time interval: 500 days before the event and 50 days after.

event ($\Delta\sigma = 44.61$ MPa) exceed the median value throughout all events, the median average value ($Me(\Delta\sigma_i) = 3.48$ MPa) in the considered time interval before the Kochkor earthquake is also lower than $Me(\Delta\sigma_{all})$ over the entire sample.

The results of computation of the median average values of stress drops $Me(\Delta\sigma_i)$ before strong and moderate earthquakes in the Northern Tien Shan are given in Table 1.

Most of the events from Table 1 during the pre-earthquake period are accompanied by a reduced value of stress drops relative to the median value over the entire sample of values.

The Southern Kuril Islands

The result obtained in the case of the Southern Kuril Islands is presented in Fig. 5. The median average value of stress drops over all events is $Me(\Delta\sigma_{all}) = 10.0$ MPa. The median average values of stress drops $\Delta\sigma_i$ before strong and moderate earthquakes in this region are given in Table 2.

A nearly 1.5-year window was used for computing the b -value parameter, however, the time behavior is gradual, because the catalog contains only events with $M > 3.6$, and there is not enough data to construct a smooth behavior curve of the b -value. Let us detail the change in the b -value and $\Delta\sigma$ during the foreshock periods for the events from Table 2 in the window of 500 days before the event and 50 after.

Fig. 6 shows the histograms of the stress drop distribution before the Shikotan earthquake of 04.10.1994, with $M = 7.9$, and the earthquake of 03.12.1995, with $M = 7.6$. As in the other seismic region, the Northern Tien Shan, there is a significant decrease in the stress drop value before the earthquake.

There is still a tendency for the increase in the slope of the recurrence plot to be accompanied by the decrease in stress drop value before an earthquake.

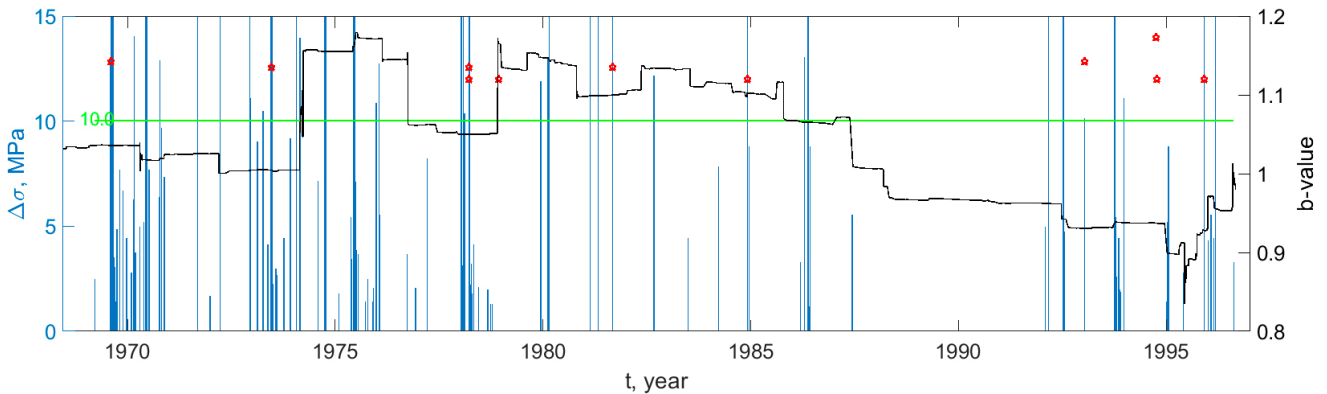


Fig. 5. The Southern Kurils. Histogram of stress drops in earthquake sources in time for the period of 1969–1996 (264 events) and the change in the b -value parameter for the considered time interval. Red stars are the events with $M \geq 6.5$. Green line is the median average stress drops over all events.

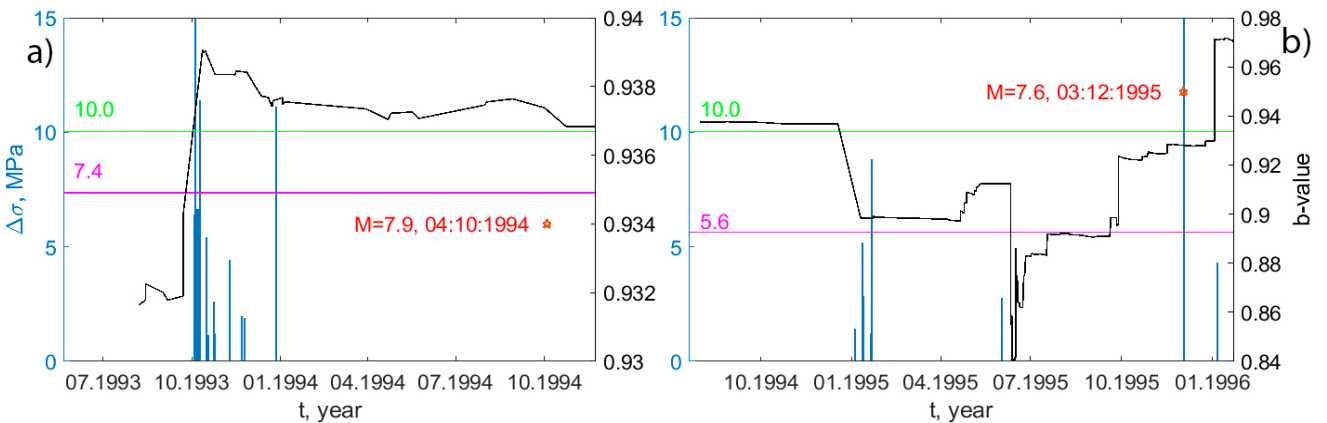


Fig 6. Stress drop histogram before the Shikotan earthquake of October 4, 1994, $M = 7.0$ (no. 10 in Table 2) (a), and the earthquake of December 3, 1995, $M = 7.6$ (no. 12 in Table 2) (b); the change in the b -value parameter. Green line is the median average value of stress drops over all events, the crimson line is the median value of stress drops for events before the earthquake. Selected time interval: 500 days before the event and 50 days after.

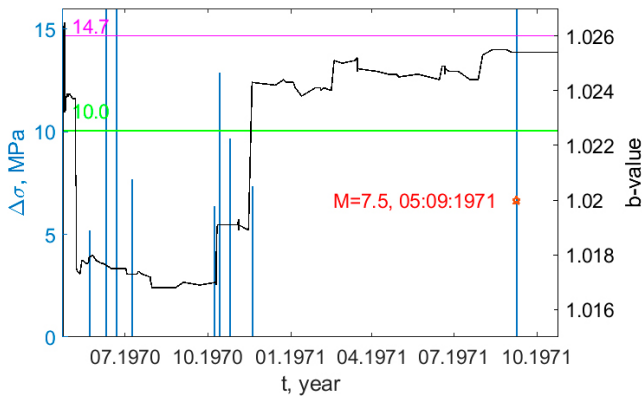


Fig. 7. Stress drop histogram before the Moneron earthquake of 05.09.1971, $M = 7.5$ and the change in the b -value parameter. Green line is the median average value of stress drops over all events, the crimson line is the median average value of stress drops for events before the earthquake. Selected time interval: 500 days before the event and 50 days after.

In the study time interval, there was another strong event – the Moneron earthquake of 05.09.1971 with $M = 7.5$ [43] (no. 2 in Table 2). However, its hypocenter was far beyond the study area: under the bottom of the Tatar Strait, a little northeast of Moneron Island, near the coast of Sakhalin Island. The hypocenter depth was 15–20 km. For all the previous observation history in the vicinity of Sakhalin Island, the earthquakes of such a great energy were not observed. The Moneron earthquake caused a tsunami [43], despite the shallow depth of this part of the Tatar Strait.

Fig. 7 shows the stress drop distribution before the Moneron earthquake of 05.09.1971 and the behavior of the b -value parameter.

The study area is more than 600 km from the epicenter of the Moneron earthquake. Despite the fact, that we have used for computations the values from the catalogs of earthquakes and dynamic parameters of events on the territory, bounded by coordinates 42° – 46° N, 144° – 151° E, and located at a significant distance from Moneron Island, an increase in the slope of recurrence plot is observed. However, there is no decrease in the stress drop value in this case. It is most likely, that the “effect” of a decrease in the stress drop value is observed in the vicinity of earthquakes, rather than at a significant distance from it.

Discussion and conclusion

The accumulation of stationary tectonic stresses, which ultimately causes the most part of earthquakes, is associated with the interaction of tectonic plates. The deformation process in the area

around the future source becomes heterogeneous and non-stationary (the characteristic period seems to correspond to the observation time of medium-term precursors: from a few months to several years) prior to strong earthquake. Spatial heterogeneity manifests itself as the stress concentration in the fault zone (in particular, on the “asperities” that prevent slipping of the fault sides) and possibly in some unloading of zones outside the concentrator localization. This can be interpreted as a decrease in the characteristic size of the stress concentration area, on which there are change in stresses and inelastic deformation processes. This seismological manifestation of change is the so-called seismic gap of the second kind, i.e. a deficit of “moderate” earthquakes with a magnitude several units less than the expected main event. The average daily number of weak earthquakes during this stage of earthquake preparation usually remains at the same level or (closer to the moment of the main event) increases. Thus, the increase in b -value parameter – the slope of the recurrence plot – gets a natural explanation [40, 41, 44]. The decrease in characteristic size can be considered as an interpretation of the above-mentioned increase in the b -value.

So, we have found the increase in the b -value parameter before strong earthquakes to be accompanied by the decrease in the median average value of stress drops $Me(\Delta\sigma_i)$. This effect was observed in two seismic regions of Eurasia: the Northern Tien Shan and the Southern Kuril Islands, and in the first case it appears more contrastingly. This is most likely due to the fact that the catalogs of dynamic parameters for the Northern Tien Shan and for the Southern Kuril Islands differ by the range of energy levels for recorded events: the Northern Tien Shan – $2.6 \leq M \leq 6.0$ [7], the Northwestern Pacific – $4.5 \leq M \leq 8.2$ [3]. When determining dynamic parameters for a wide class of events (by earthquake energies), the picture is expected to be the same.

In the case of further seismic monitoring of the considered regions, changes in the value of $\Delta\sigma$ in time can be used to reveal the non-stationary mode of the seismicity (in particular, the transition from stationary regime to the foreshock process [45]). For this purpose, it is necessary to compute dynamic parameters of the earthquake sources in a mode as close as possible to real time.

It seems that for other regions, where modern seismic networks are deployed, a massive

determination of stress drops and other dynamic parameters of earthquake source, including moderate and low energy events, is also promising. Dynamics of change in spatial distribution of stress drops can be used when forming the medium-term earthquake prediction.

References

1. Sycheva N.A., Bogomolov L.M., Kuzikov S.I. **2020**. *Computational technologies in seismological studies (on the example of KNET, Northern Tien Shan)*. Yuzhno-Sakhalinsk: IMGIG DVO RAN, 358 p. (In Russ.). <https://dx.doi.org/10.30730/978-5-6040621-6-6.2020-2>
2. Kal'met'eva Z.A., Mel'nikova T.A., Musienko E.V., Yudahin F. Ya. **1992**. [Models of source zones of strong earthquakes]. In: [Typical geological and geophysical models of seismic and aseismic regions]. Bishkek: Ilim, p. 124–131. (In Russ.).
3. Burymskaya R.N. **2001**. [Radiation spectral content and the source parameters of earthquake in the northwestern Pacific during 1969–1996]. In: A.I. Ivashchenko (ed.) [Dynamics of source zones and forecast of the strong earthquakes in the Northwestern Pacific]. Yuzhno-Sakhalinsk: IMGIG DVO RAN, vol. 1: 48–67. (In Russ.).
4. Klyuchevskii A.V., Demjanovich V.M. **2002**. Source amplitude parameters of strong earthquakes in the Baikal seismic zone. *Izv., Physics of the Solid Earth*, 38(2): 139–148. EDN: LHLKPZ
5. Brune J.N. **1970**. Tectonic stress and the spectra of seismic shear waves from earthquakes. *J. of Geophysical Research*, 75(26): 4997–5009. <https://doi.org/10.1029/jb075i026p04997>
6. Brune J.N. **1971**. Corrections. *J. of Geophysical Research*, 76: 5002.
7. Sycheva N.A., Bogomolov L.M. **2020**. On the stress drop in North Eurasia earthquakes source-sites versus specific seismic energy. *Geosistemy perhodnykh zon = Geosystems of Transition Zones*, 4(4): 393–446. (In Russ. & Engl.). <https://doi.org/10.30730/gtr.2020.4.4.393-416.417-446>
8. Dziewonski A.M., Chou T.A., Woodhouse J.H. **1981**. Determination of earthquake source parameters from waveform data for studies of regional and global seismicity. *J. of Geophysical Research*, 86: 2825–2852. <https://doi.org/10.1029/jb086ib04p02825>
9. Kocharyan G.G. **2012**. About the radiative efficiency of earthquakes (example of geomechanical interpretation of seismological observation results). *Dynamic processes in the geospheres*, 3: 36–47. (In Russ.).
10. Kocharyan G.G. **2014**. Scale effect in seismotectonics. *Geodynamics & Tectonophysics*, 5(2): 353–385. (In Russ.). <https://doi.org/10.5800/GT-2014-5-2-0133>
11. Kocharyan G.G. **2016**. *Geomechanics of faults*. Moscow: GEOS, 424 p. (In Russ.).
12. Kocharyan G.G., Ivanchenko G.N., Kishkina S.B. **2016**. Energy radiated by seismic events of different scales and genesis. *Izv., Physics of the Solid Earth*, 52(4): 606–620. <https://doi.org/10.1134/s1069351316040030>
13. Bogomolov L.M., Sycheva N.A., Zakupin A.S., Kamevnev P.A., Sychev V.N. **2015**. Stress drop distribution in sources of earthquakes and trigger effects manifestation. In: [Trigger effects in geosystems: Proceedings of the Third All-Russian workshop-meeting (Moscow, 16–19 June, 2015), IDG RAS]. Moscow: GEOS, p. 48–56. (In Russ.).
14. Sycheva N.A. **2020**. Seismic moment tensor and dynamic parameters of earthquakes in the Central Tien Shan: translation. *Geosistemy perhodnykh zon = Geosystems of Transition Zones*, 4(2): 178–209. (In Russ. & Engl.). <https://doi.org/10.30730/gtr.2020.4.2.178-191.192-209>
15. Molnar P., Tapponnier P. **1975**. Cenozoic tectonics of Asia: Effects of a continental collision: features of recent continental tectonics in Asia can be interpreted as results of the India-Eurasia collision. *Science*, 189(4201): 419–426. <https://doi.org/10.1126/science.189.4201.419>
16. Sycheva N.A. **2022**. Some characteristics of the earthquake catalog and the seismic process according to the KNET network. *Geodynamics & Tectonophysics*, 13(3). (In Russ.). <https://doi.org/10.5800/GT-2022-13-3-0640>
17. Nusipov E.H., Ospanov A.M., Li A.N., Nysanbaev T.E. **2004**. Lugovskoe earthquake May 23, 2003. In: [Modern geodynamics and seismic risk in Central Asia: Reports of the Fifth Kazakh-Chinese International Symposium, September 24–27, 2003]. Almaty: IS MON RK, p. 19–25. (In Russ.).
18. Grebennikova V.V., Frolova A.G., Bagmanova N.H., Beryozina A.V., Pershina E.V., Moldobekova S. **2018**. Kadji-Say earthquake (November 14, 2014) with $K=13.7$, $M_{pVA}=6.2$, $I_0=7$ (Kyrgyzstan – Southern Issyk-Kul). *NRC RK Bulletin*, 2(June): 135–143. (In Russ.). <https://doi.org/10.52676/1729-7885-2018-2-135-143>
19. Fortuna A.B., Abdieva S.V., Klokov I.A., Korzhenkov A.M., Strel'nikov A.A. **2019**. [Seismicity of Issyk-Kul region]. *Vestnik Instituta seismologii NAN KR [Bull. of the Institute of Seismology of the National Academy of Sciences of the Kyrgyz Republic]*, 2(14): 98–107. (In Russ.). https://journal.seismo.kg/archive/journal_2019-14/article11.pdf
20. Guseva I.S., Arkhipova E.V. **2019**. [Analysis of the system unity of the modern development of the Kuril-Kamchatka Island Arc and Sakhalin Island on the basis of seismological data]. *Uspekhi sovremennogo estestvoznaniya = Advances in Current Natural Sciences*, 6: 46–50. (In Russ.).
21. Prytkov A.S., Vasilenko N.F., Frolov D.I. **2017**. Recent geodynamics of the Kuril subduction zone. *Russian J. of Pacific Geology*, 11(1): 19–24.
22. Tihonov I.N., Levin B.V. **2015**. [Forecast of strong earthquakes in the Sakhalin region: history, results and prospects]. [Geodynamic processes and natural disasters. Experience of Neftegorsk: Sat. materials of the All-Russian scientific conference with international participation (ed. by B.V. Levin, O.N. Likhacheva)]. In 2 vol. Yuzhno-Sahalinsk; Vladivostok: Dal'nauka, vol. 1: 41–45. (In Russ.).
23. Safonov D.A., Konovalov A.V. **2017**. Moment tensor inversion in the Kuril-Okhotsk and Sakhalin regions using ISO-LA software. *Tikhookeanskaya Geologiya*, 36(3): 102–112. (In Russ.).
24. *International Seismological Centre ISC-EHB: Event catalogue*. URL: <http://www.isc.ac.uk/citations/> (accessed: 02.11.2022).
25. Kostrov B.V. **1975**. *Focal mechanics of a tectonic earthquake*. Moscow: Nauka, 175 p. (In Russ.).
26. Riznichenko Yu.V. **1985**. [Problems of seismology]. In: *Izbrannye trudy [Selected works]*. Moscow: Nauka, 408 p. (In Russ.).
27. Madariaga R. **1976**. Dynamics of an expanding circular fault. *Bull. of the Seismological Society of America*, 66: 639–666.
28. Madariaga R. **1979**. On the relation between seismic moment and stress drop in the presence of stress and strength heterogeneity. *J. of Geophysical Research*, 84: 2243–2250. <https://doi.org/10.1029/jb084ib05p02243>
29. Boore D.M. **2003**. Simulation of ground motion using the stochastic method. *Pure and Applied Geophysics*, 160(3): 635–676. <https://doi.org/10.1007/pl00012553>

30. Abercrombie R.E., Rice J.R. **2005**. Can observations of earthquake scaling constrain slip weakening? *Geophysical J. International*, 162: 406–424. <https://doi.org/10.1111/j.1365-246x.2005.02579.x>
31. Lancieri M., Madariaga R., Bonilla F. **2012**. Spectral scaling of the aftershocks of the Tocopilla 2007 earthquake in northern Chile. *Geophysical J. International*, 189: 469–480. <https://doi.org/10.1111/j.1365-246X.2011.05327.x>
32. Kaneko Y., Shearer P.M. **2014**. Seismic source spectra and estimated stress drop derived from cohesive zone models of circular subshear rupture. *Geophysical J. International*, 197(2): 1002–1015. <https://doi.org/10.1093/gji/ggu030>
33. Gibowicz S.J., Kijko A. (eds) **1994**. *An introduction to mining seismology*. San Diego: Academic Press, 399 p. <https://doi.org/10.1016/c2009-0-02348-4>
34. Moskvina A.G. **1969**. [The displacement field of elastic waves formed by propagating dislocation]. *Izvestiya AN SSSR. Fizika Zemli*, 6: 3–10. (In Russ.).
35. Moskvina A.G. **1969**. [Studies of the displacement fields of elastic waves depending on characteristics of earthquake source]. *Izvestiya AN SSSR, Fizika Zemli*, 9: 3–16. (In Russ.).
36. Sato T., Hirasawa T. **1973**. Body wave spectra from propagating shear cracks. *J. of Physics of the Earth*, 21: 415–431. <https://doi.org/10.4294/jpe1952.21.415>
37. Kwiatek G., Ben-Zion Y. **2013**. Assessment of *P* and *S* wave energy radiated from very small shear-tensile seismic events in a deep South African mine. *J. of Geophysical Research: Solid Earth*, 118(7): 3630–3641. <https://doi.org/10.1002/jgrb.50274>
38. Gutenberg B., Richter C.F. **1944**. Frequency of earthquakes in California. *Bull. of the Seismological Society of America*, 34: 185–188. <https://doi.org/10.1785/bssa0340040185>
39. Smirnov V.B., Zavyalov A.D. **2012**. Seismic response to electromagnetic sounding of the Earth's lithosphere. *Izv., Physics of the Solid Earth*, 48(7): 615–639. <https://doi.org/10.1134/s1069351312070075>
40. Smirnov V.B., Ponomaryov A.V. **2020**. *Physics of transitional regimes of seismicity*. Moscow: RAN, 412 p. (In Russ.).
41. Popandopoulos G.A. **2018**. Detailed study of time variations in the Gutenberg–Richter *b*-value based on highly accurate seismic observations at the Garm prognostic site, Tajikistan. *Izv., Physics of the Solid Earth*, 54(4): 612–631. <https://doi.org/10.1134/s1069351318040092>
42. Lyubushin A.A. **2007**. *Analysis of data from geophysical and environmental monitoring systems*. Moscow: Nauka, 228 p. (In Russ.).
43. Shchetnikov N.A. **1981**. *Tsunami*. Moscow: Nauka, 88 p. (In Russ.).
44. Tikhonov I.N. **2006**. [Earthquake catalog analysis methods for medium- and short-term predictions of strong seismic events]. Vladivostok; Yuzhno-Sakhalinsk: IMGIG DVO RAN, 214 p. (In Russ.).
45. Bogomolov L.M., Sycheva N.A. **2022**. Earthquake predictions in XXI century: prehistory and concepts, precursors and problems. *Geosistemy perekhodnykh zon = Geosystems of Transition Zones*, 6(3): 145–182. (In Russ. & Engl.). <https://doi.org/10.30730/gtr.2022.6.3.145-164.164-182>

APPENDIX

ПРИЛОЖЕНИЕ

Dynamic parameters of earthquakes in the Southern Kurils Динамические параметры землетрясений Южных Курил

The Table has been formed by the catalog of source parameters of earthquake in the Northwestern Pacific [3] as refined sampling for the territory of highest seismicity but without Hokkaido Island.

The table presents: date, time, hypocenter coordinates (φ – latitude, λ – longitude), H – depth, M_w – moment magnitude, $\lg M_0$ – decimal logarithm of scalar seismic moment, $\Delta\sigma$ – stress drops.

Таблица составлена по материалам каталога динамических параметров землетрясений северо-восточной части Тихого океана [3] как выборка для территории с наиболее высокой сейсмичностью (не включая о. Хоккайдо).

Представлены: дата, время, координаты гипоцентра (φ – широта, λ – долгота), H – глубина, M_w – моментная магнитуда, $\lg M_0$ – десятичный логарифм скалярного сейсмического момента, $\Delta\sigma$ – сброс напряжений.

No.	Date	Hour: min	φ°	λ°	H , km	M_w	$\lg M_0$, N·m	$\Delta\sigma$, МПа
1	18.03.1969	16:16	45.0	150.6	50	5.8	17.8	4.97
2	01.08.1969	23:43	45.5	150.8	40	7.2	19.6	10.39
3	02.08.1969	00:34	45.3	151.0	20	6.1	18.1	26.09
4	11.08.1969	21:08	43.5	147.8	40	5.2	16.8	59.77
5	11.08.1969	21:21	43.3	147.9	40	4.8	16.3	4.97
6	11.08.1969	21:27	43.3	147.7	15	7.2	19.9	222.07
7	11.08.1969	21:27	43.6	147.8	40	8.7	21.2	136.93
8	12.08.1969	02:36	43.5	148.3	30	5.6	17.6	3.60
9	12.08.1969	03:33	43.1	148.0	20	6.6	19.0	1338.13
10	12.08.1969	04:53	43.1	147.8	30	6.2	18.4	28.61
11	12.08.1969	05:03	43.4	148.1	30	6.9	18.5	45.34

No.	Date	Hour: min	φ°	λ°	H , km	M_w	$\lg M_0$, N·m	$\Delta\sigma$, MPa
12	12.08.1969	05:53	43.6	148.8	30	7.1	18.8	49.72
13	12.08.1969	09:25	43.2	147.7	30	5.8	17.8	19.34
14	12.08.1969	09:33	43.4	147.7	30	6.0	18.1	13.69
15	12.08.1969	11:21	43.7	149.0	50	6.8	19.3	57.08
16	12.08.1969	13:18	43.6	148.1	5	6.0	18.1	7.02
17	12.08.1969	15:28	44.0	148.9	30	5.3	17.0	15.36
18	12.08.1969	15:49	43.6	148.7	30	5.0	16.6	2.38
19	12.08.1969	21:16	43.0	146.6	40	5.6	17.5	4.75
20	12.08.1969	21:56	43.3	147.8	20	5.5	17.4	6.12
21	12.08.1969	22:57	44.0	148.4	40	6.3	18.6	8.25
22	12.08.1969	23:06	43.6	148.0	35	5.7	17.7	15.01
23	13.08.1969	03:29	43.6	147.6	40	5.7	17.7	12.20
24	13.08.1969	08:31	43.8	148.0	50	6.5	18.9	20.25
25	13.08.1969	12:30	43.2	148.1	40	4.9	16.4	3.21
26	13.08.1969	19:33	43.8	147.9	50	5.3	17.0	4.43
27	13.08.1969	22:57	44.0	148.4	40	6.5	18.9	5.58
28	14.08.1969	14:19	43.2	147.7	40	7.0	18.6	58.41
29	15.08.1969	04:32	43.3	147.8	30	6.2	18.4	55.78
30	15.08.1969	06:18	43.3	147.8	20	5.2	16.9	17.24
31	15.08.1969	09:47	43.4	147.6	20	5.1	16.8	6.12
32	15.08.1969	10:02	43.1	148.3	30	6.6	18.6	164.63
33	15.08.1969	22:43	43.2	147.5	40	5.2	16.8	15.01
34	16.08.1969	09:03	43.9	148.5	40	5.3	17.1	4.43
35	16.08.1969	12:44	43.9	148.3	40	5.3	17.0	3.36
36	16.08.1969	15:15	43.3	147.5	60	5.9	17.9	17.64
37	16.08.1969	17:13	43.2	147.6	50	5.6	17.5	8.44
38	18.08.1969	11:43	43.7	148.6	50	5.5	17.3	42.32
39	19.08.1969	08:49	43.6	148.2	40	6.2	18.4	55.78
40	21.08.1969	00:28	43.2	148.2	5	5.1	16.6	2.22
41	21.08.1969	03:32	42.9	147.1	30	5.5	17.3	50.87
42	21.08.1969	13:24	43.6	148.1	20	5.5	17.3	42.32
43	27.08.1969	01:10	43.3	147.8	30	5.1	16.6	2.22
44	27.08.1969	03:26	43.2	147.8	30	5.3	17.0	5.21
45	28.08.1969	21:35	43.2	147.8	20	5.3	17.0	18.90
46	30.08.1969	07:11	43.7	147.8	30	6.5	18.9	32.85
47	30.08.1969	08:28	43.5	147.8	25	6.0	18.1	19.79
48	04.09.1969	21:12	43.8	147.4	40	5.6	17.5	7.02
49	06.09.1969	07:43	43.8	147.4	40	5.4	17.1	6.55
50	07.09.1969	18:43	43.4	148.2	40	5.2	16.9	4.14
51	13.09.1969	11:52	43.5	147.7	50	5.2	16.9	2.61
52	14.09.1969	06:11	43.3	147.5	40	5.0	16.6	6.12
53	18.09.1969	11:52	43.3	147.1	30	5.2	16.9	2.80
54	22.09.1969	02:35	43.5	147.6	40	5.2	16.7	2.38
55	29.09.1969	17:58	43.3	147.7	40	5.4	17.4	9.69
56	26.10.1969	19:15	43.7	148.1	50	5.7	17.6	15.36

No.	Date	Hour: min	φ°	λ°	H , km	M_w	$\lg M_0$, N·m	$\Delta\sigma$, MPa
57	20.11.1969	21:00	43.4	147.9	40	5.3	17.0	13.38
58	21.11.1969	08:12	43.7	147.8	40	5.4	17.1	13.08
59	21.11.1969	08:57	43.2	147.9	35	5.0	16.6	5.21
60	19.12.1969	04:30	43.2	147.9	30	5.4	17.1	8.84
61	28.12.1969	04:53	43.4	147.7	30	5.4	17.1	8.84
62	04.02.1970	13:07	43.3	147.9	30	5.2	16.8	5.58
63	04.02.1970	20:05	44.5	148.2	25	4.1	15.2	2.80
64	26.02.1970	23:06	43.3	147.7	25	5.8	17.8	8.64
65	26.02.1970	23:29	43.3	147.8	45	5.6	17.5	8.25
66	27.02.1970	01:45	43.2	147.8	10	5.6	17.5	52.06
67	27.02.1970	02:50	43.3	147.8	40	4.4	15.7	2.07
68	10.03.1970	04:58	44.7	149.0	70	6.4	15.6	7.52
69	18.04.1970	23:25	42.9	147.4	30	5.6	17.5	9.92
70	23.05.1970	23:09	43.6	148.0	30	5.1	16.6	10.39
71	10.06.1970	16:17	44.8	149.7	40	6.7	19.2	41.35
72	22.06.1970	21:33	43.5	147.6	50	6.0	18.2	49.72
73	09.07.1970	12:11	43.8	148.4	30	6.0	17.7	15.36
74	08.10.1970	23:36	43.8	147.5	45	5.6	17.4	12.78
75	14.10.1970	16:00	43.3	148.0	40	5.1	16.8	7.19
76	14.10.1970	18:06	43.6	147.8	30	5.2	16.9	5.98
77	14.10.1970	18:15	43.4	148.0	40	6.3	18.5	21.21
78	14.10.1970	21:14	43.5	147.0	40	6.2	18.4	12.78
79	26.10.1970	19:15	43.7	148.1	50	5.6	17.4	19.34
80	20.11.1970	13:48	43.6	146.8	45	5.1	16.7	14.67
81	09.09.1971	23:01	44.3	151.0	30	6.9	19.5	44.31
82	26.12.1971	14:20	43.3	148.0	25	5.0	16.5	3.36
83	25.03.1972	22:59	43.0	146.2	45	6.8	19.3	58.41
84	10.12.1972	18:26	44.5	149.5	20	6.7	19.1	35.20
85	17.12.1972	00:18	44.5	149.5	50	5.8	17.9	22.21
86	17.02.1973	19:15	45.0	148.8	130	5.0	16.6	18.05
87	05.04.1973	22:17	43.4	147.8	41	6.0	18.0	16.09
88	06.04.1973	00:01	43.4	147.8	30	6.0	18.2	3.28
89	06.04.1973	01:48	44.2	147.2	25	5.6	17.5	19.34
90	18.05.1973	10:36	44.5	149.4	55	4.9	16.5	8.25
91	17.06.1973	03:55	43.2	145.8	50	7.7	20.6	197.92
92	18.06.1973	05:37	42.5	146.6	45	5.1	16.8	10.15
93	18.06.1973	17:45	42.3	146.1	25	6.0	18.1	14.34
94	19.06.1973	02:54	42.7	146.1	50	5.2	17.0	6.55
95	22.06.1973	06:07	42.9	146.3	53	6.5	18.9	62.59
96	23.06.1973	02:09	43.1	147.3	50	5.0	16.5	9.47
97	24.06.1973	02:43	43.4	146.5	57	7.6	20.5	1.76
98	24.06.1973	03:28	43.2	146.8	20	5.7	17.6	20.25
99	26.06.1973	18:02	43.2	147.1	50	6.7	19.1	49.72
100	26.06.1973	22:32	43.2	146.7	50	6.9	19.4	140.12
101	27.06.1973	03:42	42.8	145.7	40	4.9	16.4	3.28

No.	Date	Hour: min	φ°	λ°	H , km	M_w	$\lg M_0$, N·m	$\Delta\sigma$, MPa
102	29.06.1973	03:26	43.3	145.8	55	5.9	17.9	2.55
103	05.07.1973	00:58	43.8	148.1	30	5.2	16.8	4.53
104	29.07.1973	14:51	43.0	146.8	30	5.1	16.7	5.98
105	03.08.1973	19:13	43.0	147.8	40	4.8	16.2	4.53
106	09.08.1973	10:44	43.5	146.5	57	5.5	17.4	5.33
107	07.10.1973	09:27	42.5	146.5	15	4.8	16.3	8.84
108	01.12.1973	10:38	43.1	146.3	40	5.5	17.3	7.35
109	01.12.1973	23:16	43.1	147.1	30	5.7	19.2	5.71
110	01.12.1973	23:18	43.3	146.7	55	7.4	20.2	13.69
111	24.01.1974	19:12	42.1	144.0	30	6.7	19.4	44.31
112	25.02.1974	05:46	43.9	147.9	40	6.0	18.2	27.96
113	04.08.1974	15:00	42.4	145.9	5	5.6	17.5	14.34
114	27.09.1974	05:47	43.1	146.7	40	7.3	20.1	153.64
115	09.10.1974	07:32	44.7	150.3	50	7.3	20.0	67.07
116	02.02.1975	16:17	44.3	147.1	150	4.6	16.0	3.60
117	18.05.1975	22:34	44.2	147.7	105	5.9	17.9	10.88
118	27.05.1975	06:41	44.1	148.3	50	4.9	16.4	6.86
119	10.06.1975	13:47	43.2	147.5	30	7.6	20.4	42.32
120	10.06.1975	14:37	42.9	147.9	27	6.6	19.0	32.85
121	10.06.1975	14:58	43.9	147.8	30	6.6	19.0	43.30
122	10.06.1975	15:21	43.5	147.3	25	6.4	18.7	22.21
123	11.06.1975	14:20	43.3	147.8	15	5.3	17.0	3.86
124	11.06.1975	15:32	43.3	147.8	15	5.2	16.9	4.43
125	12.06.1975	23:21	43.1	148.0	20	5.6	17.4	8.84
126	13.06.1975	01:45	42.7	147.5	25	4.9	16.5	2.80
127	13.06.1975	12:57	43.1	147.3	24	5.1	16.7	2.43
128	13.06.1975	18:08	43.3	148.0	20	7.1	19.8	127.79
129	14.06.1975	02:59	43.1	147.8	30	5.7	17.7	7.52
130	14.06.1975	03:05	43.1	147.6	30	6.1	17.7	31.37
131	14.06.1975	05:02	43.4	147.8	30	5.7	17.7	3.95
132	14.06.1975	08:43	43.3	147.9	30	5.6	17.4	7.88
133	14.06.1975	09:02	43.3	147.7	29	4.7	16.1	7.88
134	14.06.1975	17:11	43.2	147.7	30	5.0	16.5	7.70
135	14.06.1975	17:37	43.1	147.2	24	6.1	18.3	21.70
136	14.06.1975	18:38	43.5	148.0	30	6.7	19.1	47.48
137	14.06.1975	18:49	43.4	147.9	30	6.1	18.3	11.13
138	14.06.1975	18:52	43.1	147.9	30	5.9	18.0	7.88
139	14.06.1975	20:35	43.7	147.8	24	5.1	16.7	4.64
140	14.06.1975	23:35	43.7	147.8	24	4.8	16.4	5.71
141	15.06.1975	00:19	43.2	148.0	29	7.1	19.8	82.51
142	20.06.1975	03:37	43.3	147.8	30	4.7	16.1	2.27
143	22.06.1975	01:50	43.3	147.8	30	4.7	16.1	2.27
144	22.06.1975	02:29	42.9	147.4	30	6.2	18.3	55.78
145	22.06.1975	22:44	42.9	147.4	30	6.7	19.1	49.72
146	22.06.1975	23:00	43.0	147.4	20	6.2	18.4	20.73

No.	Date	Hour: min	φ°	λ°	H , km	M_w	$\lg M_0$, N·m	$\Delta\sigma$, MPa
147	23.06.1975	09:13	43.1	147.2	25	6.4	18.4	36.02
148	26.06.1975	10:32	43.1	148.0	23	5.4	17.1	13.38
149	26.06.1975	13:07	42.9	148.2	30	5.1	16.7	7.52
150	09.07.1975	11:34	43.2	147.4	20	5.5	17.3	7.70
151	20.07.1975	08:02	44.2	148.0	80	5.6	17.5	7.35
152	24.09.1975	09:51	43.2	147.7	40	4.3	15.5	2.80
153	13.10.1975	11:51	43.0	147.8	20	4.6	16.0	4.97
154	24.11.1975	07:58	43.3	147.7	30	5.8	17.0	2.80
155	03.12.1975	07:14	43.2	145.9	50	4.9	16.4	4.14
156	27.12.1975	07:41	43.1	147.2	40	5.9	17.9	21.70
157	21.01.1976	10:05	44.8	149.1	55	7.1	19.7	22.21
158	22.01.1976	08:07	44.4	149.5	27	6.2	18.4	25.50
159	25.01.1976	12:23	44.8	149.7	60	7.2	19.8	11.13
160	22.09.1976	00:16	44.9	149.2	75	6.6	19.1	7.35
161	08.12.1976	19:19	43.3	147.9	30	6.1	18.3	4.14
162	19.03.1977	10:56	44.2	148.3	50	6.5	18.9	16.46
163	13.01.1978	20:03	44.6	150.0	40	6.5	18.8	18.90
164	14.01.1978	03:24	44.5	149.6	31	6.7	19.6	39.49
165	24.01.1978	05:54	44.6	149.3	24	6.5	18.8	6.26
166	29.01.1978	02:05	45.9	149.2	159	5.3	17.1	88.41
167	09.02.1978	08:02	44.3	150.1	30	6.6	19.0	20.73
168	22.03.1978	00:50	44.0	149.0	40	7.0	19.6	150.14
169	22.03.1978	08:25	43.8	149.3	30	5.0	16.5	4.86
170	22.03.1978	21:34	43.8	149.3	36	7.1	19.8	32.85
171	23.03.1978	00:30	44.2	149.0	40	8.1	21.3	65.54
172	23.03.1978	01:49	43.7	149.0	35	6.4	18.8	26.09
173	23.03.1978	03:14	44.2	149.8	30	6.1	19.3	40.41
174	23.03.1978	03:15	43.9	148.9	40	7.7	20.7	62.59
175	23.03.1978	07:32	44.0	148.9	40	4.7	16.0	3.00
176	23.03.1978	08:14	44.2	149.1	30	6.2	18.4	9.69
177	23.03.1978	16:52	44.0	149.4	40	4.7	16.2	5.09
178	23.03.1978	19:12	44.0	149.9	40	7.4	20.2	22.21
179	24.03.1978	22:08	43.8	149.3	40	5.8	17.8	13.69
180	24.03.1978	19:47	44.2	148.6	40	7.7	20.6	73.54
181	25.03.1978	05:24	43.9	149.4	40	4.9	16.4	5.71
182	25.03.1978	08:01	43.8	149.3	40	4.8	16.3	6.86
183	25.03.1978	23:52	43.8	148.6	40	5.6	17.4	3.52
184	26.03.1978	06:00	44.3	149.8	35	5.0	16.6	4.23
185	26.03.1978	23:56	43.7	149.2	30	5.1	16.8	5.33
186	28.03.1978	21:13	43.8	148.6	20	4.8	16.3	4.33
187	28.03.1978	22:12	43.8	148.6	20	5.7	17.6	3.14
188	05.04.1978	16:04	43.7	148.7	35	5.2	16.9	4.43
189	12.04.1978	01:22	44.1	147.8	87	5.8	17.8	6.40
190	18.04.1978	11:43	43.9	149.2	40	5.7	17.6	3.60
191	01.05.1978	06:54	44.0	149.1	35	4.9	16.4	5.09

No.	Date	Hour: min	φ°	λ°	H , km	M_w	$\lg M_0$, N·m	$\Delta\sigma$, MPa
192	01.05.1978	17:59	43.9	149.0	30	5.1	16.7	5.71
193	15.06.1978	09:28	44.1	149.2	40	5.6	17.6	4.23
194	03.09.1978	22:12	43.9	149.5	40	5.7	17.7	3.95
195	29.09.1978	11:07	43.8	149.1	35	5.0	16.6	2.61
196	11.10.1978	10:26	44.4	148.9	50	5.0	16.6	2.61
197	14.12.1979	07:19	43.0	144.4	40	6.3	18.5	23.80
198	15.02.1980	14:25	44.7	149.6	53	6.6	19.1	26.09
199	18.02.1980	06:08	43.7	146.1	110	6.2	18.4	15.01
200	23.02.1980	05:51	43.5	146.6	40	7.4	20.2	18.05
201	23.02.1980	22:38	43.2	146.9	39	6.7	19.2	32.85
202	19.02.1981	19:36	44.6	149.5	42	6.1	18.3	32.85
203	30.04.1981	14:41	43.4	150.1	30	7.0	19.6	32.85
204	03.09.1981	05:35	43.6	147.1	45	7.3	20.0	140.12
205	03.09.1982	01:32	44.0	148.4	40	6.7	19.1	24.35
206	30.06.1983	13:39	44.1	147.8	38	6.4	18.8	8.84
207	24.03.1984	09:44	44.0	148.3	42	8.0	21.1	15.72
208	03.12.1984	04:08	44.1	148.3	53	6.6	19.3	41.35
209	17.12.1984	23:30	44.5	149.8	39	6.5	18.8	17.64
210	14.03.1986	08:42	44.0	147.6	78	5.0	16.6	6.55
211	16.04.1986	12:52	44.0	147.5	43	6.8	19.4	26.09
212	21.05.1986	05:47	44.4	148.3	64	6.7	19.1	124.88
213	31.05.1986	03:40	43.8	145.5	80	4.4	15.6	2.38
214	08.06.1986	11:02	43.0	146.5	64	6.3	18.5	17.64
215	13.06.1987	14:00	44.6	150.4	43	6.4	18.7	11.13
216	02.02.1992	17:43	45.4	150.8	44	6.0	18.0	9.92
217	05.02.1992	05:33	45.7	150.6	38	5.3	17.0	8.44
218	03.03.1992	03:11	44.3	149.0	32	6.0	18.0	37.71
219	10.07.1992	09:31	44.8	149.5	33	6.3	18.5	46.50
220	12.07.1992	02:11	44.1	147.2	54	5.9	17.9	16.85
221	12.07.1992	13:14	44.6	149.7	34	6.0	18.0	22.21
222	17.07.1992	04:19	45.0	150.2	40	5.7	17.5	9.47
223	15.01.1993	11:05	43.0	144.3	82	7.6	20.4	20.25
224	04.10.1993	13:22	43.7	147.6	30.35	8.2	21.3	99.20
225	04.10.1993	18:09	43.5	147.6	33	5.5	17.3	4.33
226	04.10.1993	18:22	43.4	148.3	33	5.0	16.5	7.70
227	04.10.1993	19:16	43.7	147.4	33	5.5	17.3	7.35
228	04.10.1993	20:01	43.8	147.7	33	5.8	17.8	15.36
229	04.10.1993	20:06	43.5	147.0	33	4.9	16.2	3.86
230	04.10.1993	21:39	44.4	148.4	30	5.1	16.5	3.95
231	05.10.1993	00:02	43.3	147.8	33	4.6	16.0	2.43
232	05.10.1993	04:00	45.6	147.9	52	6.8	19.2	86.40
233	05.10.1993	07:16	42.9	148.1	29	5.8	17.8	12.20
234	05.10.1993	12:34	43.8	148.3	33	5.0	16.6	4.43
235	06.10.1993	07:38	43.3	148.6	33	5.4	17.1	5.71
236	06.10.1993	23:20	44.3	148.7	33	4.6	16.0	1.76

No.	Date	Hour: min	φ°	λ°	H , km	M_w	$\lg M_0$, N·m	$\Delta\sigma$, MPa
237	07.10.1993	02:36	43.5	147.5	31	4.8	16.2	3.86
238	07.10.1993	07:00	43.2	147.0	33	5.4	17.2	9.92
239	07.10.1993	15:00	42.7	148.0	32	5.6	17.4	7.35
240	08.10.1993	05:28	43.2	146.8	33	5.5	17.3	10.39
241	09.10.1993	07:55	43.8	148.1	35	7.9	21.0	62.59
242	09.10.1993	08:07	43.8	148.2	30	6.2	18.4	14.01
243	09.10.1993	08:49	43.8	148.3	30	5.8	17.7	10.63
244	09.10.1993	12:24	43.8	147.6	30	4.9	16.4	6.12
245	16.10.1993	05:09	45.5	149.5	180	5.9	17.7	10.88
246	18.10.1993	10:42	44.6	148.7	100	4.4	15.6	2.27
247	24.10.1993	19:27	44.0	148.4	52	5.2	16.9	5.21
248	25.10.1993	13:30	43.3	146.7	30	4.9	16.2	2.43
249	09.11.1993	18:21	43.8	147.7	100	5.1	16.7	8.84
250	22.11.1993	11:12	44.1	147.3	90	5.1	16.8	3.95
251	25.11.1993	08:49	43.3	148.9	60	5.2	16.8	3.77
252	27.12.1993	20:43	45.0	149.2	33	6.0	18.0	22.21
253	04.01.1995	23:14	43.3	147.5	33	4.8	16.3	2.86
254	12.01.1995	10:27	43.9	147.2	50	5.6	17.5	10.39
255	13.01.1995	03:13	43.2	147.0	33	5.4	17.1	5.71
256	20.01.1995	03:35	43.4	146.7	55	4.8	16.2	2.43
257	21.01.1995	08:47	43.4	146.9	60	6.3	18.4	17.64
258	02.06.1995	16:33	43.5	147.6	30	4.7	16.1	5.58
259	03.12.1995	18:01	44.7	149.3	33	7.6	20.8	279.58
260	06.01.1996	15:28	45.4	151.0	33	5.3	17.0	8.64
261	31.01.1996	20:30	44.5	149.4	21	5.9	18.0	11.13
262	22.02.1996	14:59	45.1	148.7	140	5.9	18.0	8.84
263	09.03.1996	16:15	43.4	148.0	27	6.4	18.7	38.59
264	17.08.1996	06:29	44.5	148.2	110	5.5	17.2	6.55

Об авторах

About the Authors

Богомолов Леонид Михайлович (<https://orcid.org/0000-0002-9124-9797>), доктор физико-математических наук, директор, Институт морской геологии и геофизики Дальневосточного отделения Российской академии наук, Южно-Сахалинск, bleom@mail.ru

Сычев Владимир Николаевич (<https://orcid.org/0000-0001-7508-9087>), кандидат физико-математических наук, старший научный сотрудник Центра коллективного пользования, Институт морской геологии и геофизики Дальневосточного отделения Российской академии наук, Южно-Сахалинск, koitash@mail.ru

Сычева Найля Абдуллоевна (<https://orcid.org/0000-0003-0386-3752>), кандидат физико-математических наук, старший научный сотрудник, Институт физики Земли им. О.Ю. Шмидта Российской академии наук, Москва, ivtran@mail.ru

Bogomolov, Leonid M. (<https://orcid.org/0000-0002-9124-9797>), Doctor of Physics and Mathematics, Director, Institute of Marine Geology and Geophysics of the Far Eastern Branch of RAS, Yuzhno-Sakhalinsk, bleom@mail.ru

Sychev, Vladimir N. (<https://orcid.org/0000-0001-7508-9087>), Candidate of Sciences (Physics and Mathematics), Senior Researcher, Center for Collective Use, Institute of Marine Geology and Geophysics of the Far Eastern Branch of RAS, Yuzhno-Sakhalinsk, koitash@mail.ru

Sycheva, Naylya A. (<https://orcid.org/0000-0003-0386-3752>), Candidate of Sciences (Physics and Mathematics), Senior Researcher, Schmidt Institute of Physics of the Earth of RAS, Moscow, ivtran@mail.ru

Поступила 11.01.2023

После доработки 20.02.2023

Принята к публикации 26.02.2023

Received 11 January 2023

Revised 20 February 2023

Accepted 26 February 2023